

Fluctuation-dissipation theorem and the discovery of distinctive off-equilibrium signatures of brain states

Juan Manuel Monti ^{1,2,*} Yonatan Sanz Perl ^{3,4,5} Enzo Tagliazucchi ^{6,7}
Morten L. Kringelbach ^{8,9,10} and Gustavo Deco ^{3,11}

¹*Instituto de Física Rosario CONICET-UNR, Rosario, Argentina*

²*Laboratorio de Colisiones Atómicas, FCEIA, Universidad Nacional de Rosario, Rosario, Argentina*

³*Center for Brain and Cognition, Computational Neuroscience Group, Universitat Pompeu Fabra, Barcelona, Spain*

⁴*Departamento de Matemática y Ciencias, Universidad de San Andrés, Buenos Aires, Argentina*

⁵*National Scientific and Technical Research Council (CONICET), Ciudad Autónoma de Buenos Aires, Argentina*

⁶*Physics Department, University of Buenos Aires, and Buenos Aires Physics Institute, Argentina*

⁷*Latin American Brain Health Institute (BrainLat), Universidad Adolfo Ibáñez, Santiago, Chile*

⁸*Centre for Eudaimonia and Human Flourishing, Linacre College, University of Oxford, Oxford, United Kingdom*

⁹*Department of Psychiatry, University of Oxford, Oxford, United Kingdom*

¹⁰*Center for Music in the Brain, Department of Clinical Medicine, Aarhus University, Aarhus, Denmark*

¹¹*Institució Catalana de la Recerca i Estudis Avançats (ICREA), Barcelona, Spain*



(Received 6 May 2024; revised 9 October 2024; accepted 20 February 2025; published 21 March 2025)

The brain is able to sustain many different states as shown by the daily natural transitions between wakefulness and sleep. Yet, the underlying complex dynamics of these brain states are essentially in nonequilibrium. Here, we develop a thermodynamical formalism based on the off-equilibrium extension of the fluctuation-dissipation theorem (FDT) together with a whole-brain model. This allows us to investigate the nonequilibrium dynamics of different brain states and more specifically to apply this formalism to wakefulness and deep sleep brain states. We show that the off-equilibrium thermodynamical signatures of brain states are significantly different in terms of the overall level of differential and integral violation of FDT. Furthermore, the framework allows for a detailed understanding of how different brain regions and networks are contributing to the off-equilibrium signatures in different brain states. Overall, this framework shows great promise for characterizing and differentiating brain states in health and disease.

DOI: [10.1103/PhysRevResearch.7.013301](https://doi.org/10.1103/PhysRevResearch.7.013301)

I. INTRODUCTION

A central problem in neuroscience is not only defining and characterizing brain states but also discovering the underlying mechanisms. Additionally, brain states usually refer to distinct patterns of neural activity that occur during different conditions, such as wakefulness, sleep, and anesthesia [1–4]. Moving beyond such correlational definitions, Massimini and colleagues conducted a set of highly influential experiments using direct perturbations of the brain in different states to measure the dissipation of brain activity after perturbations [5–7]. This allowed them to assess the brain-wide spatiotemporal propagation of external stimulation using the perturbational complexity index (PCI), which measures the amount of information contained in the amplitude of the average perturbation-evoked responses. PCI is computed as

the Lempel-Ziv complexity in space and time of evoked EEG signals [5].

Thermodynamics has emerged as a promising framework for understanding nonequilibrium brain dynamics by describing the information flow by using the concepts of production entropy, the arrow of time, and irreversibility to measure the asymmetry resulting from the breaking of the detailed balance in different brain states [8–11].

Importantly, here we use thermodynamics in nonequilibrium, which differs greatly from classical equilibrium thermodynamics. Our framework consists thus not in describing how particles bounce around in the brain, but instead in measuring the feedback and feed-forward information flow from interconnected neural circuits [12,13] (see also [14] and references therein). This remark is very important since brains are highly structured electromagnetic systems in nonequilibrium, and thus very unlike the classical thermodynamic notion of homogeneous heat baths consisting of a liquid of noncharged particles.

Here, we show that the fluctuation-dissipation theorem (FDT) in nonequilibrium can lead to an even better understanding of the underlying mechanisms of the perturbational results from Massimini and colleagues. It has already been shown that the violation of the FDT can describe the different

*Contact author: monti@ifir-conicet.gov.ar

Published by the American Physical Society under the terms of the [Creative Commons Attribution 4.0 International](https://creativecommons.org/licenses/by/4.0/) license. Further distribution of this work must maintain attribution to the author(s) and the published article's title, journal citation, and DOI.

levels of nonequilibrium dynamics associated with different brain states through applying Onsager’s regression principle and observing the evolution of the different brain areas following a perturbation [15]. More generally, here we adopt the off-equilibrium extension of the FDT [16–18] to develop a model-based analytical framework in which we only use data from the unperturbed system to capture deviations from equilibrium dynamics arising in different brain states. These deviations directly serve as distinctive markers of brain states.

We used this off-equilibrium FDT framework on empirical human neuroimaging data of wakefulness and deep sleep. In contrast to Massimini’s perturbational framework, we do not need to empirically perturb the brain but can directly show significantly different off-equilibrium thermodynamical signatures of brain states in terms of the overall level of differential and integral violation of FDT. Furthermore, the framework also allows for a more detailed understanding of how different brain regions and networks contribute to the off-equilibrium signatures in different brain states.

II. OFF-EQUILIBRIUM FDT

A way of expressing the FDT is through the relation between the linear response function and the autocorrelation function. The linear response function of an observable x of the system to a small enough perturbation h is given by (see [19])

$$x(t) = \int_{t'}^t dt' R(t, t') h(t'), \quad (1)$$

whereas the autocorrelation of x is defined as

$$C(t, t') = \langle x(t)x(t') \rangle, \quad (2)$$

where $\langle \dots \rangle$ states for the ensemble average. The FDT states that, if a system is in equilibrium, the linear response function is related to the autocorrelation function of the spontaneous (unperturbed) observable by

$$R(t, t') = \beta \frac{\partial C(t, t')}{\partial t'}, \quad (3)$$

where $t' \leq t$, and $\beta = 1/T$, T being the temperature of the thermal bath. The minimum distance between t' and t is given by the sampling time that, in the case of the fMRI data used in this work, is equal to 2 s. However, if the system is out of equilibrium, the generalized relation between linear response and autocorrelation is given by (see [16])

$$R(t, t') = \beta X(t, t') \frac{\partial C(t, t')}{\partial t'}. \quad (4)$$

In (4) $X(t, t')$ is called the fluctuation-dissipation ratio and characterizes the approach to equilibrium and measures the deviation from FDT. Also, as introduced in [17], a way to measure the separation from FDT, and therefore from equilibrium, is through the differential violation $V(t, t')$, and integral violation $I(t, t')$ of FDT given by

$$V(t, t') = \frac{\partial C(t, t')}{\partial t'} - T R(t, t') \quad (5)$$

and

$$I(t, t') \equiv \int_{t'}^t V(t, s) ds = C(t, t) - C(t, t') - T \chi(t, t'), \quad (6)$$

respectively, where $\chi(t, t') \equiv \int_{t'}^t R(t, s) ds$ is the integrated response function, or dynamic susceptibility. For systems in equilibrium $X = 1$, $V = 0$, and $I = 0$.

If we now consider a system evolving with the Langevin equation,

$$\frac{dx}{dt} = -F[x](t) + \eta(t), \quad (7)$$

where F is a deterministic function and $\eta(t)$ is a zero-mean Gaussian noise with autocorrelation $\langle \eta(t)\eta(t') \rangle = 2T \delta(t - t')$, we can also obtain the linear response through the expressions (see [16])

$$R(t, t') = \frac{1}{2T} \left[\frac{\partial C(t, t')}{\partial t'} - \frac{\partial C(t, t')}{\partial t} - A(t, t') \right], \quad (8)$$

$$R(t, t') = \frac{1}{2T} \langle x(t)\eta(t') \rangle, \quad (9)$$

where $A(t, t')$ is the so-called asymmetry

$$A(t, t') \equiv \langle F[x](t)x(t') - F[x](t')x(t) \rangle. \quad (10)$$

Therefore, if a system is governed by Langevin dynamics, it is possible to determine $C(t, t')$ and then $R(t, t')$ with Eqs. (8) or (9), and evaluate its distance from FDT using $X(t, t')$, $V(t, t')$, and $I(t, t')$. The degree of nonequilibrium determined by the distance from FDT could then be a marker of brain states (e.g., wakefulness, sleep, coma). To prove this hypothesis, we use empirical human neuroimaging data (fMRI, functional Magnetic Resonance Imaging) for wakefulness and deep sleep, in order to fit a whole-brain model that can be written as a Langevin equation to simulate data from which the linear response $R(t, t')$ can be calculated using Eqs. (8) or (9) to further determine $X(t, t')$, $V(t, t')$, and $I(t, t')$.

III. WHOLE-BRAIN MODEL

Previous research has proposed that different brain states are characterized by different dynamical regimes [20,21]. As a matter of fact, it was shown that at the macroscopic and microscopic scales, unconscious brain states are dominated by synchronous activity [20–24]. In contrast, conscious states are characterized by asynchronous dynamics [21,25,26]. Aligned with this, we consider a whole-brain model consisting of N coupled brain regions (nodes) where the local dynamic of each brain region is described using a Hopf bifurcation in its normal form (also known as a Stuart-Landau oscillator) (see [27]) and has extensively been used to successfully fit empirical neuroimaging signals (e.g., [2,28]).

With this, each node can present an asynchronous noisy state or display coherent oscillations when being below or above a given threshold, respectively. Then, each node j of the brain network is modeled by a normal Hopf bifurcation as

$$\frac{dz_j}{dt} = z_j[a_j + i\omega_j - |z_j|^2] + \sigma \eta_j(t). \quad (11)$$

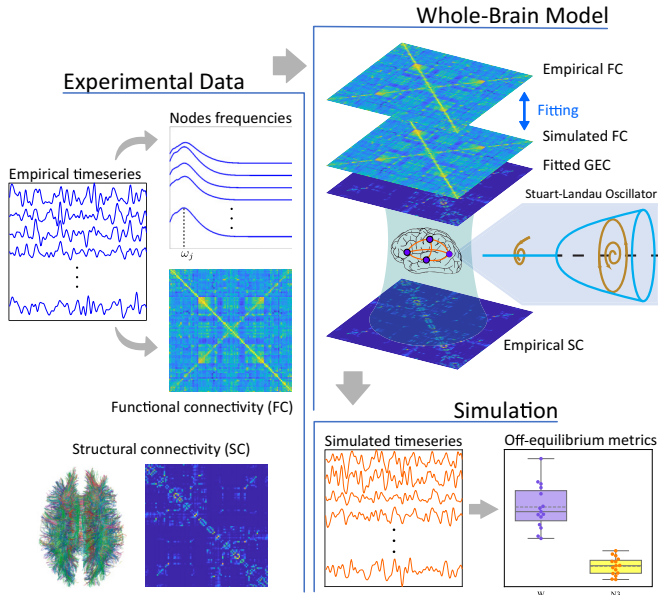


FIG. 1. Model-based nonequilibrium FDT. Using empirical data we link anatomical connectivity and functional brain connectivity in order to fit a Hopf whole-brain model to generate simulated data that satisfies Eq. (7). The simulated data is then used to determine the distance from equilibrium using Eqs. (15)–(17).

In (11) a_j is the so-called bifurcation parameter, ω_j the node frequency, and $\sigma \eta_j(t)$ is a zero-mean additive Gaussian noise with standard deviation σ . We then consider the coupling of the network nodes through the anatomical network as given by the generative effective connectivity matrix (GEC) $\tilde{\mathbf{C}}$. The GEC matrix is initialized using the empirical structural connectivity (SC, obtained with probabilistic tractography from dMRI) and is then optimized as shown in the Supplemental Material [29] and Refs. [30–33] therein. Hence, the whole-brain dynamics is modeled via the following set of coupled equations:

$$\frac{dx_j}{dt} = (a_j - x_j^2 - y_j^2)x_j - \omega_j y_j + \sum_i \tilde{C}_{ij}(x_i - x_j) + \sigma \eta_j(t), \quad (12)$$

$$\frac{dy_j}{dt} = (a_j - x_j^2 - y_j^2)y_j + \omega_j x_j + \sum_i \tilde{C}_{ij}(y_i - y_j) + \sigma \eta_j(t), \quad (13)$$

where x_j is the simulated signal for each node j . Then, the whole-brain model given by Eqs. (12) and (13) can be written as a set of coupled Langevin equations.

Model parameters: Fitting of the Hopf whole-brain model to empirical data

The empirical fMRI BOLD data, to which the whole-brain model is fitted (see Fig. 1), is constituted of two cohorts corresponding to wakefulness and deep sleep (N3 stage of sleep) brain states, each composed of 15 individual scans (subjects), with $N = 90$ nodes corresponding to the AAL90 parcellation, and $n_F = 180$ time frames (see the Supplemental Material

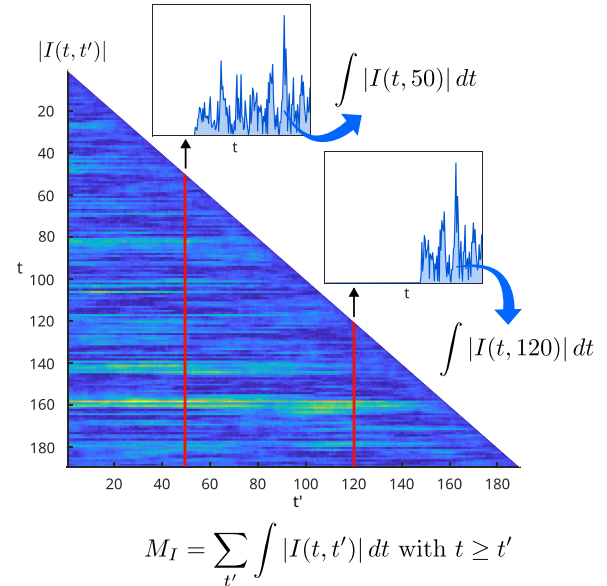


FIG. 2. Calculations of metrics. Typical subdiagonal matrix obtained for $|I(t, t')|$ for one brain region. For each timestep t' (showing $t' = 50$ and $t' = 120$ as examples), we calculate the mean over t (with $t \geq t'$) and the sum over all t' to obtain the different metrics.

[29] and Refs. [34–42] therein). The only fixed parameter in the model is the local bifurcation parameter which is set to the value $a_j = -0.02$ for all subjects and the different brain states considered. As stated in [43], this corresponds to all the oscillators being at the brink of the bifurcation. The node frequencies ω_j , for each brain state, are determined as the peak of the mean power spectrum of the empirical time series [27]. Finally, the standard deviation σ of the Gaussian noise is obtained by searching for the value of σ that gives the least difference between the empirical and simulated matrices defined as

$$\overline{\mathbf{C}}(t, t') = \overline{x(t)x(t')}; \quad (14)$$

here the bar means performing the average over all the subjects in each given brain state (see the Supplemental Material [29]).

IV. APPLYING THE FORMALISM TO WAKEFULNESS AND DEEP SLEEP BRAIN STATES

Once the whole-brain model is fitted to each subject, simulated time series can be obtained, from which autocorrelation [Eq. (2)], and the linear response [Eqs. (8) or (9)] can be calculated. For each subject, and each node, we can obtain three $n_F \times n_F$ subdiagonal matrices (X, V, and I) and define three metrics to determine the distance from equilibrium (see Fig. 2), i.e., the deviation from FDT, namely,

$$M_{X_j} = \sum_{t'} \int |(X_j(t, t') - 1)| dt, \quad (15)$$

$$M_{V_j} = \sum_{t'} \int |V_j(t, t')| dt, \quad (16)$$

$$M_{I_j} = \sum_{t'} \int |I_j(t, t')| dt; \quad (17)$$

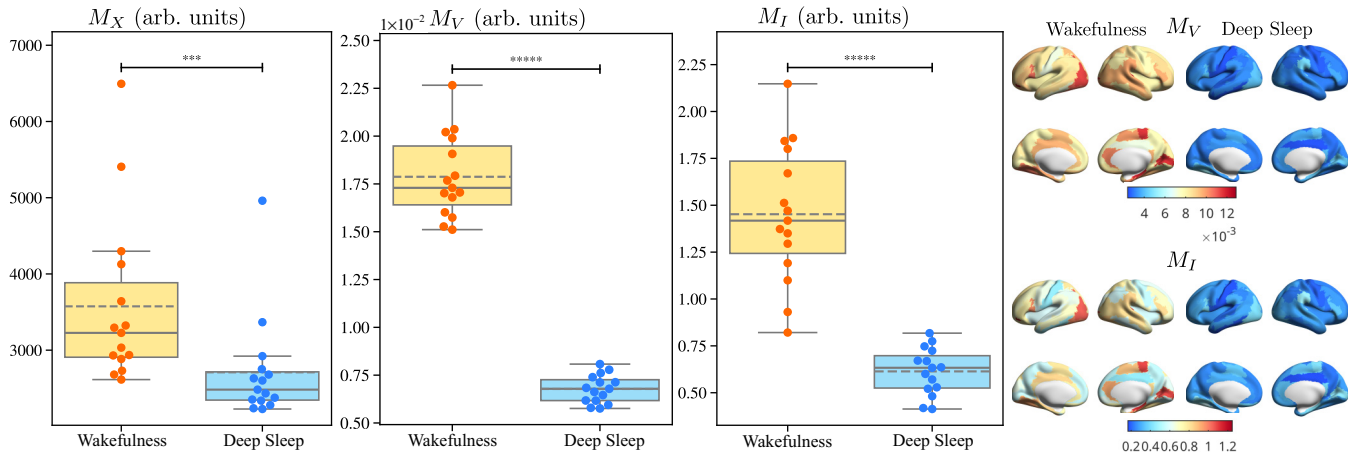


FIG. 3. Nonequilibrium characterization of brain states. Boxplots: metrics across subjects. Deviation from FDT, i.e., distance from equilibrium calculated as the average for all nodes for each subject using the metrics M_X [Eq. (15)] (left), M_V [Eq. (16)] (center), and M_I [Eq. (17)] (right). Solid lines represent the median of the distributions, whilst the dashed lines indicate their mean. Brain plots: metrics across brain areas. Here we also consider averaging over subjects instead of nodes, hence the level of nonequilibrium can be studied for each region on the wakefulness (left) and deep-sleep states (right).

each of these metrics can give a measure of the distance from the equilibrium of the brain region j . Then, for each subject, we can take the average over all nodes as a more global indicator of distance from equilibrium.

V. BRAIN STATES CHARACTERIZATION

In Fig. 3, we show the average over all the brain regions for each subject in the wakefulness and deep sleep groups. The ensemble average was determined by performing 10 000 simulations for each subject and each brain state. A discussion about the convergence of the metrics with respect to the number of simulations can be found in the Supplemental Material [29]. In general, all three metrics show a higher departure from equilibrium for the wakefulness group, with statistical significance $p < 1e^{-3}$ for M_X , and $p < 1e^{-5}$ for M_V and M_I (calculated with a Wilcoxon rank-sum test) between the distributions. Also for the differential and integral violations of FDT, there is no overlapping between the swarmplots which shows high distinguishability between states.

The distribution plots in all cases show more spreading in the wakefulness group, whereas the deep sleep distribution appears more clustered. This aspect may reflect the fact that the deep-sleep state has less intersubject variability than wakefulness.

Of the three metrics given, the one that gives more reliable results is the M_I one, as it does not depend on the numerical derivation of a noisy function. Instead, it involves an integration, which is numerically much more reliable. Also, it shows the fastest convergence with respect to the number of simulations (see the Supplemental Material [29]).

On the other hand, if instead of performing an average over the nodes, a mean over subjects is considered, we can obtain the deviation from equilibrium for each brain region, which is shown in Fig. 3. This could be used to determine the intrinsic hierarchy of brain regions that characterize different brain states.

We have also directly compared the present framework to two other classical methods (LZ complexity and autocorrelation windows, as shown in the Supplemental Material [29] and Refs. [44–48] therein). This comparison shows that the present framework is clearly more sensitive to distinguishing between wakefulness and sleep.

VI. DISCUSSION

We have presented a model-based formalism using the Hopf whole-brain model together with the off-equilibrium generalization of the FDT theorem presented in [16], with which the spontaneous simulated time series can be used to determine the departure from equilibrium of different brain states.

The present framework provides us with the opportunity to introduce novel metrics that aid in identifying and labeling brain states and providing a direct thermodynamic measure. As such, this is an addition to the many existing observational and perturbational metrics used to characterize levels of wakefulness [49–52]. These could be combined to provide the best classification of a given brain state if this is the goal. Still, here we concentrate on simply quantifying the power of our thermodynamic framework which allows us to distinguish the features of brain dynamics with both high specificity and sensitivity, whilst allowing us to delve deeper into the relationship between brain activity and the physical concept of nonequilibrium [16–18].

This formalism offers a dynamical systems explanation showing that feedback-loops are key for awareness as suggested by Lamme and colleagues [14] and their idea that the feedback and feed-forward connections in brains at all scales. This could be a reason for why small perturbations in our FDT framework determine the distance from equilibrium which can sensitively distinguish brain states.

It is important to emphasize that this work does not suggest a direct correspondence between the physical variables of a thermodynamic system and brain activity measurements.

While the fluctuation-dissipation theorem (FDT) originates from nonequilibrium thermodynamics, our results demonstrate that the mathematical formalism of FDT provides a useful framework for characterizing whole-brain activity, capturing key dynamical properties without necessarily implying a direct correspondence with physical thermodynamic principles. Rather than asserting a strict physical analogy, we emphasize that FDT serves as a powerful analytical tool for identifying distinctive signatures of brain states within a well-defined mathematical structure.

The results also show that there is a clear distinction between the wakefulness and deep sleep states based on their distance from equilibrium determined by the metrics derived from the fluctuation-dissipation ratio [16], the differential and the integral violations of FDT [17]. More precisely, we found that the deviations from equilibrium were larger in the wakefulness state than in deep sleep. These findings are in agreement with those from [9] where the level of nonreversibility of different brain states and cognitive tasks are evaluated in electrocorticography data from nonhuman primates showing larger levels of irreversibility for wakefulness than for deep sleep. Also (see the Supplemental Material [29] and Ref. [53] therein), present results for the M_I metric are compared with the Lempel-Ziv complexity index (LZCI) obtained for the empiric time series. The LZCI is a well-known model-free metric that has been used to study epilepsy [54], different depths of anesthesia [55], and alternate states of consciousness [56]. The comparison shows that both the LZCI and the present M_I metric can discriminate between wakefulness and deep sleep states. Nonetheless, the statistical significance is much better when using the M_I metric, which also shows no overlapping between the two states.

As stated above, there is a correspondence between the temperature of the thermal bath in which the system evolves [16] and the standard deviation of the noise in the Hopf model. This would indicate that, at least in the model, each brain state also has a characteristic noise. Following the analogy, we may think that each brain state is a different thermal bath in which the system (brain) evolves. This also sheds light on the role of noise in the model, not only present to generate transitions between the noisy and oscillatory regimes of the Hopf bifurcation but also playing a more fundamental role in defining the brain state.

The off-equilibrium FDT formalism presented here has the advantage that only data from the simulated system spontaneous activity is needed to determine the metrics that define the distance from equilibrium. This avoids the need of perturbing the system, whether experimentally or *in silico*.

Regarding the possibility of applying this formalism in a model-free approach, we could define our observable $x(t)$ as being the empirical BOLD signal of a given brain region and then impose the Langevin equation introduced in Eq. (7), i.e., numerically computing its derivative dx/dt , and then splitting the signal into its two components, the unknown operator

$F[x](t)$ and the noise $\eta(t)$ which must satisfy two key requirements: Gaussianity and delta correlation. If the empirical signals satisfy these conditions, we could proceed with the rest of the equilibrium analysis. Future research should pursue this approach which has the potential to provide valuable insights into the underlying dynamics of spontaneous brain activity.

One important point to note was raised by Bayne and colleagues [57] who argued that awareness may not be a one-dimensional construct measured by levels of awareness, but rather a multidimensional construct measured across several distinct dimensions (see Laureys *et al.* [58]).

Overall, here we provide a model-based framework that can be used to evaluate the level of nonequilibrium by determining the degree of violation of FDT through the metrics provided. This allows us to characterize distinct brain states, namely wakefulness and deep sleep. All the metrics show a larger level of nonequilibrium in the wakefulness state than in deep sleep. This is in clear alignment with the idea that nonequilibrium brain dynamics is a general feature of conscious states [11]. The model-based formalism presented here, along with the new metrics derived for quantifying nonequilibrium, is suitable not only for characterizing different conditions and brain states but also for conducting *in silico* experiments.

In future research we plan to extend this investigation by considering other brain states such as different degrees of comatose states, e.g., minimally conscious state and unresponsiveness wakefulness syndrome, diverse cognitive tasks, and different stages of neurodegenerative diseases and stroke.

It would also be of considerable interest to investigate new models, e.g., extending the important work of Sleigh and Liley [59] to the present framework with the caveat that such models must obey Langevin dynamics in order to determine the response function R with the equations presented.

ACKNOWLEDGMENTS

J.M.M. acknowledges financial support from CONICET through external scholarship for researchers. G.D. was supported by several sources: NEMESIS project (Ref. 101071900) funded by the EU ERC Synergy Horizon Europe; AGAUR research support Grant (Ref. 2021 SGR 00917) funded by the Department of Research and Universities of the Generalitat of Catalunya; and Project PID2022-136216NB-I00 financed by the MCIN /AEI /10.13039/501100011033 / FEDER, UE., the Ministry of Science and Innovation, the State Research Agency and the European Regional Development Fund. M.L.K. is supported by the Centre for Eudaimonia and Human Flourishing (funded by the Pettit and Carlsberg Foundations) and Center for Music in the Brain (funded by the Danish National Research Foundation, DNRF117). Y.S.P. is supported by European Union's Horizon 2020 research and innovation program under the Marie Skłodowska-Curie Grant 896354.

[1] D. Gervasoni, S.-C. Lin, S. Ribeiro, E. S. Soares, J. Pantoja, and M. A. L. Nicolelis, Global forebrain dynamics predict rat

behavioral states and their transitions, *J. Neurosci.* **24**, 11137 (2004).

- [2] M. L. Kringelbach and G. Deco, Brain states and transitions: Insights from computational neuroscience, *Cell Rep.* **32**, 108128 (2020).
- [3] G. Northoff, What the brain's intrinsic activity can tell us about consciousness? A tri-dimensional view, *Neurosci. Biobehav. Rev.* **37**, 726 (2013).
- [4] G. Tononi, O. Sporns, and G. M. Edelman, A measure for brain complexity: relating functional segregation and integration in the nervous system, *Proc. Natl. Acad. Sci. USA* **91**, 5033 (1994).
- [5] A. G. Casali, O. Gosseries, M. Rosanova, M. Boly, S. Sarasso, K. R. Casali, S. Casarotto, M.-A. Bruno, S. Laureys, G. Tononi, and M. Massimini, A theoretically based index of consciousness independent of sensory processing and behavior, *Sci. Transl. Med.* **5**, 198ra105 (2013).
- [6] F. Ferrarelli, M. Massimini, S. Sarasso, A. Casali, B. A. Riedner, G. Angelini, G. Tononi, and R. A. Pearce, Breakdown in cortical effective connectivity during midazolam-induced loss of consciousness, *Proc. Natl. Acad. Sci. USA* **107**, 2681 (2010).
- [7] M. Massimini, F. Ferrarelli, R. Huber, S. K. Esser, H. Singh, and G. Tononi, Breakdown of cortical effective connectivity during sleep, *Science* **309**, 2228 (2005).
- [8] G. Deco, Y. Sanz Perl, L. de la Fuente, J. D. Sitt, B. T. T. Yeo, E. Tagliazucchi, and M. L. Kringelbach, The arrow of time of brain signals in cognition: Potential intriguing role of parts of the default mode network, *Network Neuroscience* **7**, 966 (2023).
- [9] G. Deco, Y. Sanz Perl, H. Bocaccio, E. Tagliazucchi, and M. L. Kringelbach, The insideout framework provides precise signatures of the balance of intrinsic and extrinsic dynamics in brain states, *Commun. Biol.* **5**, 572 (2022).
- [10] C. W. Lynn, E. J. Cornblath, L. Papadopoulos, M. A. Bertolero, and D. S. Bassett, Broken detailed balance and entropy production in the human brain, *Proc. Natl. Acad. Sci. USA* **118**, e2109889118 (2021).
- [11] Y. Sanz Perl, H. Bocaccio, C. Pallavicini, I. Pérez-Ipiña, S. Laureys, H. Laufs, M. Kringelbach, G. Deco, and E. Tagliazucchi, Nonequilibrium brain dynamics as a signature of consciousness, *Phys. Rev. E* **104**, 014411 (2021).
- [12] V. A. Lamme, H. Supèr, and H. Spekreijse, Feedforward, horizontal, and feedback processing in the visual cortex, *Current Opin. Neurobiol.* **8**, 529 (1998).
- [13] V. A. Lamme and P. R. Roelfsema, The distinct modes of vision offered by feedforward and recurrent processing, *Trends Neurosci.* **23**, 571 (2000).
- [14] V. A. Lamme, Towards a true neural stance on consciousness, *Trends Cognit. Sci.* **10**, 494 (2006).
- [15] G. Deco, C. W. Lynn, Y. Sanz Perl, and M. L. Kringelbach, Violations of the fluctuation-dissipation theorem reveal distinct nonequilibrium dynamics of brain states, *Phys. Rev. E* **108**, 064410 (2023).
- [16] L. F. Cugliandolo, J. Kurchan, and G. Parisi, Off equilibrium dynamics and aging in unfrustrated systems, *J. Phys.* **4**, 1641 (1994).
- [17] L. F. Cugliandolo, D. S. Dean, and J. Kurchan, Fluctuation-dissipation theorems and entropy production in relaxational systems, *Phys. Rev. Lett.* **79**, 2168 (1997).
- [18] F. Corberi, E. Lippiello, and M. Zannetti, Fluctuation dissipation relations far from equilibrium, *J. Stat. Mech.* (2007) P07002.
- [19] R. Kubo, Statistical-mechanical theory of irreversible processes. I. general theory and simple applications to magnetic and conduction problems, *J. Phys. Soc. Jpn.* **12**, 570 (1957).
- [20] J. S. Goldman, N. Tort-Colet, M. di Volo, E. Susin, J. Bouté, M. Dali, M. Carlu, T.-A. Nghiem, T. Górski, and A. Destexhe, Bridging single neuron dynamics to global brain states, *Front. Syst. Neurosci.* **13**, 75 (2019).
- [21] M. V. Sanchez-Vives and D. A. McCormick, Cellular and network mechanisms of rhythmic recurrent activity in neocortex, *Nat. Neurosci.* **3**, 1027 (2000).
- [22] M. Steriade, A. Nunez, and F. Amzica, A novel slow (< 1 Hz) oscillation of neocortical neurons *in vivo*: depolarizing and hyperpolarizing components, *J. Neurosci.* **13**, 3252 (1993).
- [23] E. N. Brown, R. Lydic, and N. D. Schiff, General anesthesia, sleep, and coma, *New England J. Med.* **363**, 2638 (2010).
- [24] M. D. Fox, A. Z. Snyder, J. L. Vincent, M. Corbetta, D. C. V. Essen, and M. E. Raichle, The human brain is intrinsically organized into dynamic, anticorrelated functional networks, *Proc. Natl. Acad. Sci. USA* **102**, 9673 (2005).
- [25] M. E. Raichle, A. M. MacLeod, A. Z. Snyder, W. J. Powers, D. A. Gusnard, and G. L. Shulman, A default mode of brain function, *Proc. Natl. Acad. Sci. USA* **98**, 676 (2001).
- [26] M. Boly, C. Phillips, L. Tshibanda, A. Vanhaudenhuyse, M. Schabus, T. Dang-Vu, G. Moonen, R. Hustinx, P. Maquet, and S. Laureys, Intrinsic brain activity in altered states of consciousness, *Annu. N.Y. Acad. Sci.* **1129**, 119 (2008).
- [27] G. Deco, M. L. Kringelbach, V. K. Jirsa, and P. Ritter, The dynamics of resting fluctuations in the brain: metastability and its dynamical cortical core, *Sci. Rep.* **7**, 3095 (2017).
- [28] S. Idesis, M. Allegra, J. Vohryzek, Y. S. Perl, N. V. Metcalf, J. C. Griffis, M. Corbetta, G. L. Shulman, and G. Deco, Generative whole-brain dynamics models from healthy subjects predict functional alterations in stroke at the level of individual patients, *Brain Commun.* **6**, fae237 (2024).
- [29] See Supplemental Material at <http://link.aps.org/supplemental/10.1103/PhysRevResearch.7.013301> for further information on empiric data acquisition, model fitting, convergence of metrics, and comparison with other model-free metrics.
- [30] M. Gilson, R. Moreno-Bote, A. Ponce-Alvarez, P. Ritter, and G. Deco, Estimation of directed effective connectivity from fMRI functional connectivity hints at asymmetries of cortical connectome, *PLoS Comput. Biol.* **12**, e1004762 (2016).
- [31] M. Gilson, G. Zamora-López, V. Pallarés, M. H. Adhikari, M. Senden, A. T. Campo, D. Mantini, M. Corbetta, G. Deco, and A. Insabato, Model-based whole-brain effective connectivity to study distributed cognition in health and disease, *Network Neuroscience* **4**, 338 (2020).
- [32] M. Gilson, G. Deco, K. J. Friston, P. Hagmann, D. Mantini, V. Betti, G. L. Romani, and M. Corbetta, Effective connectivity inferred from fMRI transition dynamics during movie viewing points to a balanced reconfiguration of cortical interactions, *NeuroImage* **180**, 534 (2018), Brain Connectivity Dynamics.
- [33] M. L. Kringelbach, Y. S. Perl, E. Tagliazucchi, and G. Deco, Toward naturalistic neuroscience: Mechanisms underlying the flattening of brain hierarchy in movie-watching compared to rest and task, *Sci. Adv.* **9**, eade6049 (2023).
- [34] N. Tzourio-Mazoyer, B. Landeau, D. Papathanassiou, F. Crivello, O. Etard, N. Delcroix, B. Mazoyer, and M. Joliot, Automated anatomical labeling of activations in SPM using a

- macroscopic anatomical parcellation of the MNI MRI single-subject brain, *NeuroImage* **15**, 273 (2002).
- [35] K. Setsompop, R. Kimmlingen, E. Eberlein, T. Witzel, J. Cohen-Adad, J. McNab, B. Keil, M. Tisdall, P. Hoehn, P. Dietz, S. Cauley, V. Tountcheva, V. Matschl, V. Lenz, K. Heberlein, A. Potthast, H. Thein, J. Van Horn, A. Toga, F. Schmitt *et al.*, Pushing the limits of *in vivo* diffusion MRI for the human connectome project, *NeuroImage* **80**, 220 (2013), Mapping the Connectome.
- [36] A. Horn, W.-J. Neumann, K. Degen, G.-H. Schneider, and A. A. Kühn, Toward an electrophysiological “sweet spot” for deep brain stimulation in the subthalamic nucleus, *Human Brain Mapping* **38**, 3377 (2017).
- [37] A. Horn and F. Blankenburg, Toward a standardized structural–functional group connectome in MNI space, *NeuroImage* **124**, 310 (2016).
- [38] K. H. Maier-Hein, P. F. Neher, J.-C. Houde, M.-A. Côté, E. Garyfallidis, J. Zhong, M. Chamberland, F.-C. Yeh, Y.-C. Lin, Q. Ji, W. E. Reddick, J. O. Glass, D. Q. Chen, Y. Feng, C. Gao, Y. Wu, J. Ma, R. He, Q. Li, C.-F. Westin *et al.*, The challenge of mapping the human connectome based on diffusion tractography, *Nat. Commun.* **8**, 1349 (2017).
- [39] K. G. Schilling, A. Daducci, K. Maier-Hein, C. Poupon, J.-C. Houde, V. Nath, A. W. Anderson, B. A. Landman, and M. Descoteaux, Challenges in diffusion MRI tractography – lessons learned from international benchmark competitions, *Magn. Reson. Imaging* **57**, 194 (2019).
- [40] A. B. A. Stevner, D. Vidaurre, J. Cabral, K. Rapuano, S. F. V. Nielsen, E. Tagliazucchi, H. Laufs, P. Vuust, G. Deco, M. W. Woolrich, E. Van Someren, and M. L. Kringelbach, Discovery of key whole-brain transitions and dynamics during human wakefulness and non-rem sleep, *Nat. Commun.* **10**, 1035 (2019).
- [41] G. H. Glover, T.-Q. Li, and D. Ress, Image-based method for retrospective correction of physiological motion effects in FMRI: RETROICOR, *Magn. Reson. Med.* **44**, 162 (2000).
- [42] P. J. Allen, G. Polizzi, K. Krakow, D. R. Fish, and L. Lemieux, Identification of EEG events in the MR scanner: The problem of pulse artifact and a method for its subtraction, *NeuroImage* **8**, 229 (1998).
- [43] G. Deco and M. L. Kringelbach, Turbulent-like dynamics in the human brain, *Cell Rep.* **33**, 108471 (2020).
- [44] R. V. Raut, A. Mitra, S. Marek, M. Ortega, A. Z. Snyder, A. Tanenbaum, T. O. Laumann, N. U. F. Dosenbach, and M. E. Raichle, Organization of propagated intrinsic brain activity in individual humans, *Cereb. Cortex* **30**, 1716 (2020).
- [45] T. Watanabe, G. Rees, and N. Masuda, Atypical intrinsic neural timescale in autism, *eLife* **8**, e42256 (2019).
- [46] T. Ito, L. J. Hearne, and M. W. Cole, A cortical hierarchy of localized and distributed processes revealed via dissociation of task activations, connectivity changes, and intrinsic timescales, *NeuroImage* **221**, 117141 (2020).
- [47] C. J. Honey, T. Thesen, T. H. Donner, L. J. Silbert, C. E. Carlson, O. Devinsky, W. K. Doyle, N. Rubin, D. J. Heeger, and U. Hasson, Slow cortical dynamics and the accumulation of information over long timescales, *Neuron* **76**, 423 (2012).
- [48] M. Golesorkhi, J. Gomez-Pilar, S. Tumati, M. Fraser, and G. Northoff, Temporal hierarchy of intrinsic neural timescales converges with spatial core-periphery organization, *Commun. Biol.* **4**, 277 (2021).
- [49] G. Deco, J. Cabral, V. M. Saenger, M. Boly, E. Tagliazucchi, H. Laufs, E. Van Someren, B. Jobst, A. Stevner, and M. L. Kringelbach, Perturbation of whole-brain dynamics *in silico* reveals mechanistic differences between brain states, *NeuroImage* **169**, 46 (2018).
- [50] R. Comolatti, A. Pigorini, S. Casarotto, M. Fecchio, G. Faria, S. Sarasso, M. Rosanova, O. Gosseries, M. Boly, O. Bodart, D. Ledoux, J.-F. Brichant, L. Nobili, S. Laureys, G. Tononi, M. Massimini, and A. G. Casali, A fast and general method to empirically estimate the complexity of brain responses to transcranial and intracranial stimulations, *Brain Stimul.* **12**, 1280 (2019).
- [51] L. S. Imperatori, J. Cataldi, M. Betta, E. Ricciardi, R. A. A. Ince, F. Siclari, and G. Bernardi, Cross-participant prediction of vigilance stages through the combined use of wPLI and wSMI EEG functional connectivity metrics, *Sleep* **44**, zsa247 (2021).
- [52] Y. Sanz Perl, C. Pallavicini, I. Pérez Ipiña, A. Demertzi, V. Bonhomme, C. Martial, R. Panda, J. Annen, A. Ibañez, M. Kringelbach, G. Deco, H. Laufs, J. Sitt, S. Laureys, and E. Tagliazucchi, Perturbations in dynamical models of whole-brain activity dissociate between the level and stability of consciousness, *PLoS Comput. Biol.* **17**, e1009139 (2021).
- [53] P. E. Rapp, Quantitative characterization of animal behavior following blast exposure, *Cognitive Neurodynamics* **1**, 287 (2007).
- [54] N. Radhakrishnan and B. Gangadhar, Estimating regularity in epileptic seizure time-series data, *IEEE Eng. Med. Biol. Mag.* **17**, 89 (1998).
- [55] X.-S. Zhang, R. Roy, and E. Jensen, EEG complexity as a measure of depth of anesthesia for patients, *IEEE Trans. Biomed. Eng.* **48**, 1424 (2001).
- [56] M. M. Schartner, R. L. Carhart-Harris, A. B. Barrett, A. K. Seth, and S. D. Muthukumaraswamy, Increased spontaneous meg signal diversity for psychoactive doses of ketamine, LSD and psilocybin, *Sci. Rep.* **7**, 46421 (2017).
- [57] T. Bayne, J. Hohwy, and A. M. Owen, Are there levels of consciousness? *Trends Cognit. Sci.* **20**, 405 (2016).
- [58] S. Laureys, The neural correlate of (un)awareness: lessons from the vegetative state, *Trends Cognit. Sci.* **9**, 556 (2005).
- [59] M. L. Steyn-Ross, D. A. Steyn-Ross, J. W. Sleight, and D. T. J. Liley, Theoretical electroencephalogram stationary spectrum for a white-noise-driven cortex: Evidence for a general anesthetic-induced phase transition, *Phys. Rev. E* **60**, 7299 (1999).